Reversible Photocontrol of DNA Binding by a Designed GCN4-bZIP Protein[†]

G. Andrew Woolley,*[,‡] Anna S. I. Jaikaran,[‡] Maxim Berezovski,[§] Joseph P. Calarco,[‡] Sergey N. Krylov,[§] Oliver S. Smart,[∥] and Janet R. Kumita[‡,⊥]

Department of Chemistry, University of Toronto, 80 Saint George Street, Toronto M5S 3H6, Canada, Department of Chemistry, York University, Toronto M3J 1P3, Canada, and School of Biosciences, University of Birmingham, Edgbaston, Birmingham B15 2TT, United Kingdom

Received January 23, 2006; Revised Manuscript Received March 9, 2006

ABSTRACT: Synthetic photocontrolled proteins could be powerful tools for probing cellular chemistry. Several previous attempts to produce such systems by incorporating photoisomerizable chromophores into biomolecules have led to photocontrol but with incomplete reversibility, where the chromophore becomes trapped in one photoisomeric state. We report here the design of a modified GCN4-bZIP DNA-binding protein with an azobenzene chromophore introduced between Cys residues at positions 262 and 269 (S262C, N269C) within the zipper domain. As predicted, the trans form of the chromophore destabilizes the helical structure of the coiled-coil region of GCN4-bZIP, leading to diminished DNA binding relative to wild type. Trans-to-cis photoisomerization of the chromophore increases helical content and substantially enhances DNA binding. The system is observed to be readily reversible; thermal relaxation of the chromophore to the trans state and concomitant dissociation of the protein−DNA complex occurs with $\tau_{1/2}$ ~10 min at 37 °C. It appears that conformational dynamics in the zipper domain make the transition state for isomerization readily available so that retention of reversible switching is observed.

Using light to control the activity of biomolecules is an attractive strategy for probing interactions in complex living systems. Photosensitive biomolecules can be introduced into cells and manipulated noninvasively with a high degree of spatial and temporal control (*1*, *2*). For instance, caged compounds, in which a light flash is used to produce a step increase in the concentration of a bioactive species, have facilitated studies of muscle contraction, intracellular signaling, and neurotransmission (*3*, *4*). Whereas synthetic caged compounds undergo an essentially irreversible photochemical reaction, nature has evolved numerous *reversible* means for coupling light signals to cellular chemistry (e.g., refs *5* and *6*). Such reversible systems can produce more sophisticated sorts of temporal responses than can caged compounds. In an effort to understand the essential features of such natural photoswitches and to learn how to create synthetic photoswitches, we have taken a minimalist approach (*7*) to the design of reversible photocontrolled biomolecules.

Recently, we reported a means of controlling the stability of α-helices, common and important elements of protein secondary structure, via the incorporation of a photoisomerizable azobenzene cross-linking reagent (compound **1**; Figure 1) (*8*−*10*). The photocontrolled conformational changes in these helical systems were found to be completely reversible with relatively small effects of the peptide structure on the rate of recovery of the dark-adapted (trans) azobenzene conformation (*11*). We wished to test whether this reversibility would be maintained when the conformational change was coupled to a change in a defined biological activity such as binding to a partner biomolecule. The system we chose to study is the well-characterized bZIP DNA-binding domain of the yeast transcriptional activator, GCN4.

The GCN4-bZIP protein has a two-state folding mechanism from random coil monomers to folded helical dimers (*12*). GCN4-bZIP preferentially recognizes the seven base pair AP1 site, 5′-TGACTCA-3′ (*13*, *14*). In the absence of the cognate DNA, the leucine zipper peptide (residues 249−281) can form a stable coiled coil of parallel α-helices (*15*, *16*) whereas the basic region peptide (residues 223−248) exists as an ensemble of conformers with a large unfolded population (*17*, *18*). In the presence of cognate DNA, the bound bZIP-GCN4 proteins form a Y-shaped dimer of uninterrupted, extended α-helices as shown by X-ray crystallography (Figure 2) (*19*). The leucine zipper domain forms the stem of the dimer joined to the extended basic regions which bind to the major groove of DNA (*19*).

DNA binding of bZIP-GCN4 is dependent on two properties, the dimerization of the leucine zipper region and the direct interaction of the basic region with DNA (*19*). In pioneering work, Mascarenas and co-workers used an azobenzene-based cross-linker to artificially dimerize the basic regions of GCN4 (*20*). Artificially dimerized GCN4 basic regions have been shown to be capable of specific and high-affinity recognition of native GCN4 DNA-binding sites (*21*, *22*). The cis photoisomer was found to bind DNA more tightly than the trans isomer by gel-shift analysis. However, DNA binding was found to inhibit the cis → trans photoisomerization (and thermal isomerization) process (*20*). We

[†] Financial support from the Natural Sciences and Engineering Research Council of Canada (to G.A.W.) is gratefully acknowledged.

* To whom correspondence should be addressed. E-mail: awoolley@chem.utoronto.ca. Telephone/fax: (416) 978−0675.

[‡] University of Toronto.

[§] York University.

[∥] University of Birmingham.

[⊥] Present address: Department of Chemistry, Cambridge University, Lensfield Road, Cambridge CB2 1EW, U.K.

10.1021/bi060142r CCC: $33.50
Published on Web 04/18/2006

now report a different approach, the incorporation of an azobenzene cross-linker into the leucine zipper region of bZIP-GCN4, that results in reversible photocontrol of GCN4 DNA-binding ability.

MATERIALS AND METHODS

Site-Directed Mutagenesis. The plasmid pGCN4-56 (kindly provided by J. J. Hollenbeck and M. G. Oakley) contains the coding sequence for a 58 amino acid protein containing the 56 C-terminal residues of GCN4, preceded by the codons for Met and Lys (*23*). Site-directed mutagenesis was performed using the QuikChange site-directed mutagenesis kit (Stratagene, La Jolla, CA) to introduce two cysteine residues at an *i*, *i* + 7 spacing (S262C, N269C primer 1, 5′ GC AAC TTC GCA CTC GAG GTG GTA GTT TTT ACA CAG *C*AG GTC TTC 3′; S262C, N269C primer 2, 5′ GAA GAC CT*G* CTG TGT AAA AAC TAC CAC CTC GAG TGC GAA GTT GC 3′). Mutations resulting in an amino acid change are underlined. Note that E259 was also mutated to D259 due to the primer design. Mutations that result in removal of the *Sac*I restriction enzyme site, but do not cause a change in amino acid sequence, are denoted in italics. Mutated sequences were confirmed by automated sequencing (HSC Biotechnology Service Centre, Toronto, Canada).

Target DNA. Oligonucleotides corresponding to the AP1 site were synthesized by ACGT Corp. (Toronto, Canada). The sequence 5′-TCCGGATGACTCATTTTTTG-3′ and its complement were used. For capillary electrophoresis the reverse-phase HPLC-purified 5′-fluorescein- (FAM-) labeled analogue of this sequence (TriLink Technologies Inc., San Diego, CA) was employed. For both labeled and unlabeled cases, the oligonucleotide was mixed in a 1:1 ratio with its complementary (unlabeled) sequence and annealed using standard protocols (*24*).

Protein Expression and Purification. pGCN4-56 and pGCN4-(S262C, N269C)-56 were overexpressed in the *Escherichia coli* strain BL21(DE3)pLysS using the T7 expression system (Novagen, Madison, WI). Cells were harvested 2 h after induction by centrifugation and the cell pellets frozen until purification. Cell pellets were thawed and resuspended in 50 mM Tris-HCl (pH 7.5), 5 mM EDTA, and 1 M NaCl (40 mL of buffer for 1 L of cell culture). Cells were lysed by sonication on ice, and the lysate was centrifuged at 11000 rpm for 30 min at 4 °C. The supernatant was dialyzed against 5 mM sodium phosphate (pH 7), 10 mM $MgCl_2$, and 1:1000 β-mercaptoethanol.

The dialyzed supernatant was mixed with an equal volume of 2× column buffer [2 M NaCl, 2 M ammonium sulfate, 100 mM sodium phosphate (pH 7), 10 mM $MgCl_2$, 1 mM DTT], stirred at 4 °C for 30 min, and filtered using a 0.45 μm syringe filter unit (Millipore). The filtrate was applied to a 1 mL phenyl-Sepharose column in four separate batches. Each batch was eluted using a 10 mL gradient from buffer A [1 M NaCl, 1 M ammonium sulfate, 50 mM sodium phosphate (pH 7), 10 mM $MgCl_2$, 1 mM DTT] to buffer B [50 mM sodium phosphate (pH 7), 10 mM $MgCl_2$, 1 mM DTT] on an FPLC system (GE Healthcare).

Fractions containing GCN4 were pooled and dialyzed against 5 mM sodium phosphate (pH 7) and 1:1000 β-mercaptoethanol. The dialyzed solution was mixed with 1 M sodium phosphate (pH 7) to a final concentration of 50 mM. DTT was added to a final concentration of 1 mM. The solution was filtered, and the filtrate was applied to a 1 mL CM-Sepharose column; then fractions were eluted using a 10 mL gradient from buffer A [50 mM sodium phosphate (pH 7), 1 mM DTT] to buffer B [50 mM sodium phosphate (pH 7), 2 M NaCl, 1 mM DTT].

Fractions containing GCN4 were pooled and dialyzed against distilled water containing 1:1000 β-mercaptoethanol. The volume was reduced by half using a vacuum pump, and TCEP (Sigma) was added to 1 mM. The sample was placed in a Microcon centrifugation device and the buffer exchanged for 20 mM ammonium acetate and 1 mM TCEP. The final volume was 140 μL.

The protein primary structures were confirmed by MALDI-MS and ESI-MS: GCN4-bZIP [calculated ($C_{293}H_{510}N_{100}O_{86}S_2$) 6874.0 Da; observed 6874.4 Da]; (*i*, *i* + 7)Cys GCN4-bZIP [calculated ($C_{291}H_{507}N_{99}O_{84}S_4$) 6865.1 Da; observed 6864.2 Da]. Protein concentration was determined by measuring the tyrosine absorbance at 275 nm using a molar extinction coefficient of 1470 M^{-1} cm^{-1}.

Cross-Linking (i, i + 7)Cys GCN4-bZIP. Intramolecular cross-linking of Cys residues was performed in the presence of guanidine hydrochloride to disrupt the dimeric coiled-coil interaction of (*i*, *i* + 7)Cys GCN4-bZIP. In a total volume of 290 μL of 44 mM Tris-HCl buffer (pH 8.0), uncross-linked (*i*, *i* + 7)Cys GCN4-bZIP (0.78 mM), TCEP (0.84 mM), and GdnHCl (2.3 M) were combined and incubated for 30 min at room temperature under nitrogen to ensure the cysteine residues were in their reduced state. The aqueous solution was added to 250 μL of water containing 0.34 μmol of the cross-linker, giving a reagent concentration of 0.63 mM. This solution was stirred for 20 min protected from light in a 40 °C water bath; then a further 34 μL of a 10 mM solution of the cross-linker (**1**) was added. The reaction mixture was stirred in a 40 °C water bath for a further 20 min protected from light followed by 20 min exposed to light. The protein was purified by reverse-phase HPLC (Zorbax SB C-18 column), using a linear gradient from 0 to 50% of solvent A (90% acetonitrile + 0.1% trifluoroacetic acid) (where solvent B was H_2O with 0.1% trifluoroacetic acid), over the course of 30 min (eluted at ~50% solvent A). The protein primary structure was confirmed by MALDI-MS and ESI-MS [calculated ($C_{307}H_{519}N_{103}O_{92}S_6$) 7317.5; observed 7317 plus 7333 [Met(O)] species]. Cross-linked protein concentration was determined by measuring the absorbance of the dark-adapted azobenzene moiety at 367 nm and using a molar extinction coefficient of 24000 M^{-1} cm^{-1}.

UV and CD Measurements. Ultraviolet absorbance spectra were obtained using either a Perkin-Elmer Lambda 2 spectrophotometer modified to accept cylindrical cuvettes (so that UV could be measured directly on CD samples) or a diode array UV−vis spectrophotometer (Ocean Optics Inc., USB2000) coupled to a temperature-controlled cuvette holder (Quantum Northwest, Inc.). The latter arrangement was used to determine thermal relaxation rates of cross-linked species. Irradiation of the sample (at 90° to the light source and detector used for the absorbance measurements) was carried out using a xenon lamp (450 W) coupled to a double monochromator with slits at 16 and 16 nm. Rates of thermal cis-to-trans isomerization were measured for a series of temperatures by monitoring absorbance at 370 nm after

irradiation to convert a percentage of the solution to the cis isomer. All curves could be fit well by single exponential decay kinetics. Solution conditions are described in the figure legends.

Circular dichroism measurements were performed with a Jasco model J-710 spectropolarimeter. All measurements were taken in a thermostated quartz cuvette (path length of 0.1 cm). Temperatures were measured using a microprobe directly in the sample cell. Reported spectra are averages with the appropriate background spectrum subtracted. A scan speed of 10 nm/min, with a bandwidth of 0.5 nm and a response time of 4 s, was used. Using the percent cis observed by UV [calculated on the basis of spectra of pure cis and trans isomers (*11*)], theoretical 100% cis CD spectra were calculated using the equation $\theta_{cis} = [\theta_{irrad} - (\text{fraction trans} \times \theta_{trans})]/(\text{fraction cis})$. Photoisomerization was accomplished by irradiating thermostated protein solutions with a 70 W metal halide Tri-Lite lamp (World Precision Instruments) coupled to a 370 ± 10 nm band-pass filter (Harvard Apparatus Canada). Photoisomerization was complete (as judged by the lack of any further changes in UV spectra) in ~5 min. Solution conditions are described in the figure legends.

Analytical Ultracentrifugation. Sedimentation equilibrium experiments were carried out at the Ultracentrifugation Service Facility in the Department of Biochemistry at the University of Toronto. Solutions of between 5 and 30 μM GCN4-bZIP (wild type) and AZO(*i*, *i* + 7) GCN4-bZIP in 10 mM sodium phosphate buffer, pH 7.0, and 50 mM NaCl were spun at speeds of 30000, 35000, and 40000 rpm in an An-60 Ti rotor in a Beckman Optima XL-A analytical ultracentrifuge at 20 °C. Absorbance was recorded at 230 nm for GCN4-bZIP (wild type) and at 370 nm (the absorbance maximum of the trans cross-linker) for AZO(*i*, *i* + 7) GCN4-bZIP. Data analysis was performed using the Origin Microcal XL-A/CL-I data analysis software package version 4.0.

Kinetic Capillary Electrophoresis. Fused-silica capillaries were purchased from Polymicro (Phoenix, AZ). All solutions were made using Milli-Q quality deionized water and filtered through a 0.22 μm filter (Millipore, Nepean, Canada). Binding studies were performed with a P/ACE MDQ, Beckman-Coulter instrument with thermostabilization of the capillary (the outer walls of the capillary were washed with a liquid heat exchanger maintained at a fixed temperature) and sample vials. The instrument employed laser-induced fluorescence detection with a 488 nm line of an argon ion laser for fluorescence excitation. An uncoated fused silica capillary was used with the following dimensions: 50 cm × 75 μm i.d. × 350 μm o.d. The length from the injection end to the detection window was 40 cm. Electrophoresis was run with a positive electrode at the injection end and an electric field of 400 V/cm at 15 °C. The run buffer for all CE experiments was 50.0 mM Tris-HCl at pH 8.2. The samples were injected into the capillary by a pressure pulse of 5 s × 0.5 psi (3.5 kPa); the length of corresponding sample plug was 6 mm. The capillary was rinsed with the run buffer solution for 2 min prior to each run. At the end of each run, the capillary was rinsed with 100 mM NaOH for 2 min, followed by a rinse with deionized water for 2 min. All CE experiments were performed in three repeats. Samples were prepared by mixing protein and DNA in the incubation buffer, irradiating (or not) and incubating in the dark at the desired temperature (from 4 to 25 °C) in the CE instrument. The incubation buffer was 50 mM MOPS, pH 7.5, and 50 mM KCl, with or without 133 μg /mL calf thymus DNA, 100 μg/mL BSA, and 5% glycerol.

Computer Modeling. Models of cross-linked AZO(*i*, *i* + 7) GCN4-bZIP were built using SYBYL (Tripos) based on the X-ray crystal structure (PDB code 1YSA). The geometry of the cross-linker in cis and trans forms was optimized using the program Gaussian as described previously (*25*). Conformational searches of isolated linkers with methyl groups replacing Cys β atoms were performed using SYBYL. Systematic searches were performed by rotating all single bonds in the linker in 30° increments. Bond angles and bond lengths were taken from X-ray crystallographic studies (*26*, *27*) and high-level computational studies of azobenzene (*28*). S−S distances in transition state structures were estimated by setting the N═N bond torsion angle to 90° (rotation) or by setting one N═N−C bond angle to 180° (inversion) (*29*). Molecular dynamics simulations of the coiled-coil domain of wild-type GCN4-bZIP were performed by Gorfe et al. (*30*) using the CHARMM program. The standard protonation states of the acidic and basic groups at neutral pH were used. Histidines were treated as neutral, and N- and C-terminal residues were patched with neutral acetate and amide groups, respectively. The particle mesh Ewald method was used to treat the long-range electrostatics. Because the total charge of the protein was zero, no counterions were added. The protein was immersed in a rectangular box of dimensions 70 × 50 × 50 Å containing preequilibrated TIP3P water. After minimization, the system was equilibrated for 30 ps under isothermal (298 K), constant volume conditions applying harmonic constraints on the protein heavy atoms with a force constant of 2.0 kcal mol^{-1} Å^{-2}. The equilibrated system was heated to 298 K in 15 ps. The harmonic constraint force constant was progressively decreased from 2.0 to 0.0 kcal mol^{-1} Å^{-2} in the initial 10 ps, and all atoms were free during the last 5 ps of the heating process. The system was then subjected to a 20 ps equilibration at constant temperature and volume by using Gaussian distribution for the assignment of atomic velocities. The production simulations were performed for 0.3 and 0.7 ns.

RESULTS

Protein Design and Production. Figure 1 shows the sequence of GCN4-bZIP. On the basis of previous work with peptides (*8*) we introduced an azobenzene-based cross-linker between Cys residues with an *i*, *i* + 7 spacing. This spacing is expected to lead to helix stabilization by a cis conformation of the cross-linker and helix destabilization by a trans conformation (*8*, *10*). A sequence alignment of GCN4-bZIP with homologous protein sequences from the SWISS-PROT databank (*31*) indicated that the b, c, and f positions from the heptad repeat are most tolerant to alteration (*32*). Mutation to cysteine of two consecutive f positions in the heptad repeat would produce the required *i*, *i* + 7 spacing and would ensure that the cysteine/cross-linker/cysteine moiety would lie on the solvent-exposed side of the coiled coil (Figures 1 and 2). The only places where the desired changes could be made without altering the charge of the protein were S262C and N269C (Figure 1). To assess the compatibility of the cross-linked structure with coiled-coil

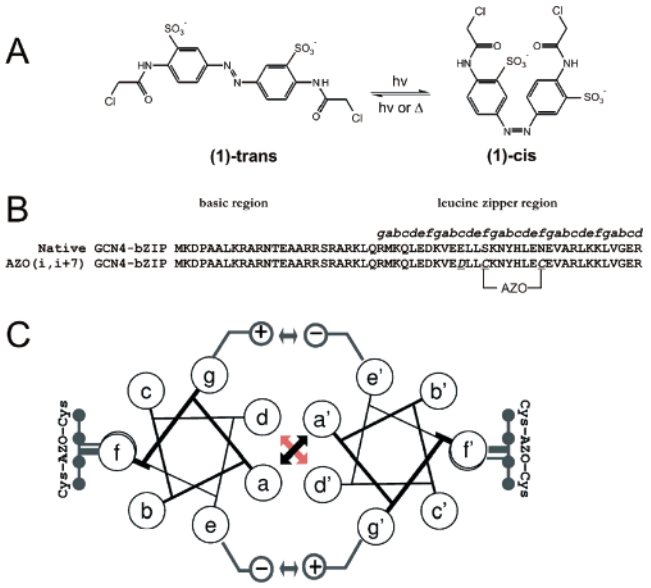

FIGURE 1: (A) Chemical structure of the azobenzene cross-linker. (B) Sequence of native GCN4-bZIP and the S262C, N269C mutant (*i*, *i* + 7)Cys GCN4-bZIP showing the attachment of the cross-linker. The heptad repeat, basic region, and coiled-coil (zipper) regions are identified. (C) Helical wheel diagram showing the leucine zipper region of the azo-modified sequence. The arrows at the center of the interface represent the hydrophobic interactions between residues in the a and d positions of the heptad repeat. The linker is introduced at f positions as indicated, and a single c position was also modified.

formation, two models were produced, one with the azobenzene group in a cis conformation and the other with the azobenzene in the trans form. The amino acid modifications were incorporated into the high-resolution X-ray crystal structure (*15*) of the isolated GCN4 leucine zipper peptide using the SYBYL package. The conformation of each form of the azobenzene cross-linker was the result of ab initio geometry optimization using the 6-31G* basis function with Gaussian 98. The GCN4-bZIP dimer structure was then separated into two monomers. For each of the monomers the cross-linker was joined to the cysteine side chains. Each cross-linked monomer was then subjected to energy minimization with the AMBER4.1 force field (*33*), while the cross-linker was constrained to its ab initio low-energy conformation. After energy minimization the two monomers modeled with the cross-linker in a cis conformation remained fully helical and could be rejoined to form a dimer. On the basis of this result, a model for a modified GCN4-bZIP with the cross-linker in a cis conformation was produced (Figure 2), based on the X-ray crystal structure for GCN4-bZIP in complex with cognate DNA. In contrast, the trans conformation of the cross-linker forced a considerable bend in the helix (Figure 2), indicating that the helical dimer was likely to be destabilized.

Native GCN4-bZIP (GCN4-bZIP wild type) and the (*i*, *i* + 7)Cys GCN4-bZIP mutant were overexpressed in *E. coli* and purified using a combination of hydrophobic interaction chromatography and ion-exchange chromatography as described in Materials and Methods. The cross-linking reagent (**1**) (Figure 1) (*34*) was introduced into (*i*, *i* + 7)Cys GCN4-bZIP at the cysteine residues, resulting in an intramolecular cross-linkage. The resulting protein, AZO(*i*, *i* + 7) GCN4-bZIP (Figure 1), was purified by HPLC and characterized by ESI-MS. In addition to the main peak there is also some protein 16 atomic mass units heavier, consistent with some oxidation of Met1 or Met27 as has been recently reported (*35*). Oxidation of Met27, in particular, might serve to decrease the average dimerization affinity of the modified protein since Met27 is at an "a" position in the heptad repeat (see below).

Conformational Properties of Azobenzene Cross-Linked GCN4 in the Absence of DNA. Figure 3A shows UV spectra of dark-adapted (trans) and irradiated (370 nm, ~1 mW, 5 min) protein solutions in the absence of DNA. The percentage of cis-AZO(*i*, *i* + 7) GCN4-bZIP present in the irradiated sample can be calculated to be ~75% on the basis of a comparison to the spectrum of the pure (isolated) cis chromophore (*10*, *34*). The extent of conversion is consistent with other studies of the azobenzene chromophore and is determined by the ground state cis and trans absorption spectra as well as the relative quantum yields of the cis → trans and trans → cis photoisomerization processes, which vary with the environment of the chromophore. The rate of recovery of the trans conformation of AZO(*i*, *i* + 7) GCN4-bZIP in the dark was studied at 25 and 37 °C. Single exponential recovery curves were observed with half-lives similar to those measured previously for dark-state recovery of the same chromophore attached to (unstructured) glutathione (Table 1) (*34*).

Circular dichroism (CD) spectroscopy provides a convenient method for assessing the degree of helical structure in peptides and proteins. CD spectra of irradiated and dark-adapted states of AZO(*i*, *i* + 7) GCN4-bZIP are shown in Figure 3B together with the spectrum for wild-type GCN4-

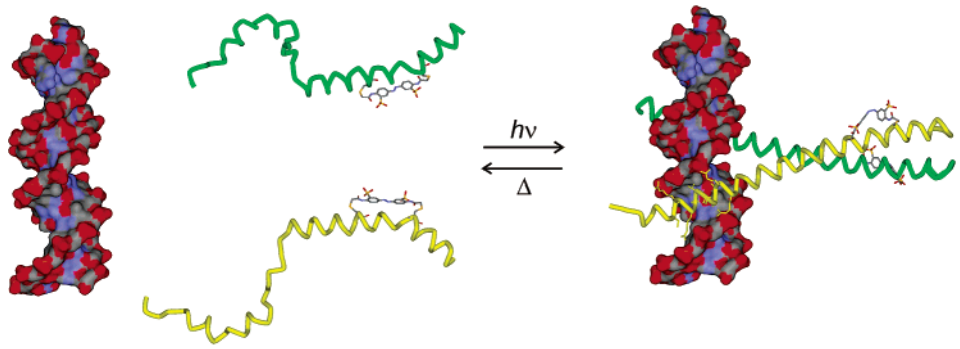

FIGURE 2: Models showing the photocontrol of DNA binding by AZO(*i*, *i* + 7) GCN4-bZIP. In the trans conformation, the cross-linker induces a bend in the helix, which can be expected to destabilize zipper formation and consequently DNA binding (left). In contrast, the cis conformation of the cross-linker is compatible with zipper formation and thus DNA binding (right).

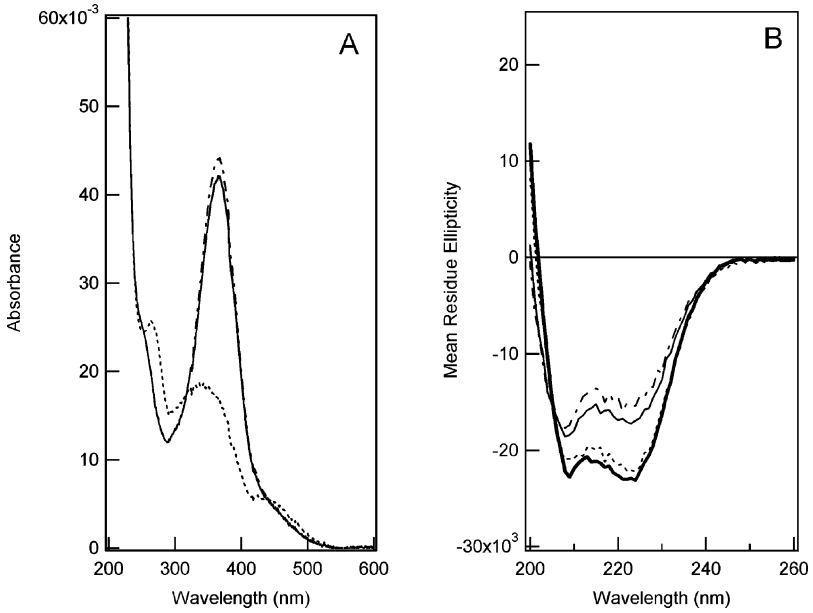

FIGURE 3: Spectroscopic analysis of AZO(*i*, *i* + 7) GCN4-bZIP. (A) UV spectra of AZO(*i*, *i* + 7) GCN4-bZIP in the dark-adapted state (solid line) and irradiated state (dotted line) and after recovery (dash−dot line). (B) CD spectra of dark-adapted AZO(*i*, *i* + 7) GCN4-bZIP (solid line), after irradiation (dotted line), and after recovery (dash−dot line). The CD spectrum of wild-type GCN4-bZIP (heavy solid line) is shown for reference. Solution conditions: 10 mM phosphate buffer, pH 7.0, and 50 mM NaCl at 10 ± 1 °C at a protein concentration of 20 μM.

Table 1

	$\tau_{1/2}$ (min)		
temp (°C)	GCN4-bZIP	plus AP1	azoglutathione
25	50 ± 3	35 ± 5	25 ± 3
37	14 ± 2	10 ± 2	12 ± 2

bZIP. Weiss et al. have reported detailed CD studies of the wild-type GCN4-bZIP domain (*17*, *36*). They observed that the CD spectrum is concentration dependent in the range of 0.1−10 μM with the protein showing increased helicity with increased concentration up to a maximum of approximately 70% helix ($\theta_{222} = -22700$ deg cm^2 dmol^{-1}) at 25 °C. This behavior has been attributed to dimerization and helical coiled-coil formation by the zipper domain with the DNA-binding domain remaining unstructured (*17*).

The CD spectrum of the dark-adapted (trans) form of AZO(*i*, *i* + 7) GCN4-bZIP shows significantly less helicity (47%) than wild-type GCN4-bZIP under the same conditions (Figure 3B). Moreover, the observed helicity is independent of concentration over the range of 1−50 μM, indicating that the aggregation state of trans AZO(*i*, *i* + 7) GCN4-bZIP does not change over this concentration range. Interestingly, however, this degree of helicity is substantially more than for wild-type GCN4-bZIP at low concentrations where the protein is monomeric.

To investigate the aggregation state of trans AZO(*i*, *i* + 7) GCN4-bZIP, we performed analytical ultracentrifugation measurements on wild-type GCN4-bZIP (MW 6876) and trans AZO(*i*, *i* + 7) GCN4-bZIP (MW 7317). Figure 4 shows a sedimentation equilibrium analysis of these two proteins at a concentration of 20 μM in 10 mM sodium phosphate buffer, pH 7.0, and 50 mM NaCl at 20 °C. Under these conditions trans AZO(*i*, *i* + 7) GCN4-bZIP is predominantly monomeric with an average apparent molecular weight of 8450 whereas wild-type GCN4-bZIP is predominantly dimeric with an average apparent molecular weight of 12650.

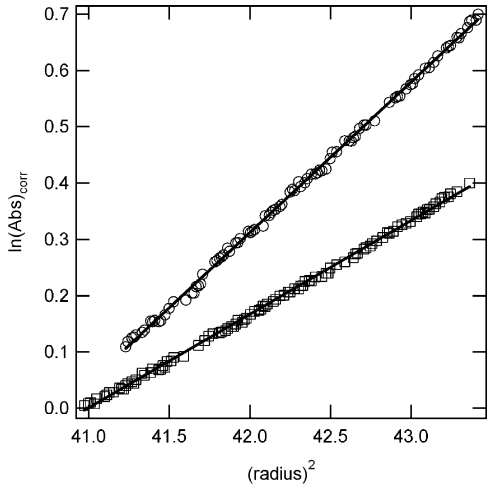

FIGURE 4: Sedimentation equilibrium analysis of wild-type GCN4-bZIP (○) and AZO(*i*, *i* + 7) GCN4-bZIP (□) at 20 °C in the same solution conditions as used for the CD experiments. Plots of ln-(Abs) (offset so that the axis starts at zero) versus radius^2 are linear, indicating the presence of predominantly one species in each case. Calculated average molecular weights: wild-type GCN4-bZIP (12650) and AZO(*i*, *i* + 7) GCN4-bZIP (8450).

It thus appears that cross-linking with a trans cross-linker preserves substantial residual helical structure in the monomeric protein, even though it is locally incompatible with helix formation, a result consistent with previous studies of cross-linked zipper domain peptides (*32*).

Irradiation of the AZO(*i*, *i* + 7) GCN4-bZIP CD sample at 370 nm produces a substantial increase in helicity resulting in an overall spectrum very similar to that observed for the wild-type (dimeric) protein. The shape of the spectrum is consistent with the presence of a dimeric form of the protein (*37*); however, it was not possible to perform analytical ultracentrifugation studies to determine the aggregation state of the irradiated form of AZO(*i*, *i* + 7) GCN4-bZIP directly since the time required for sedimentation equilibrium is

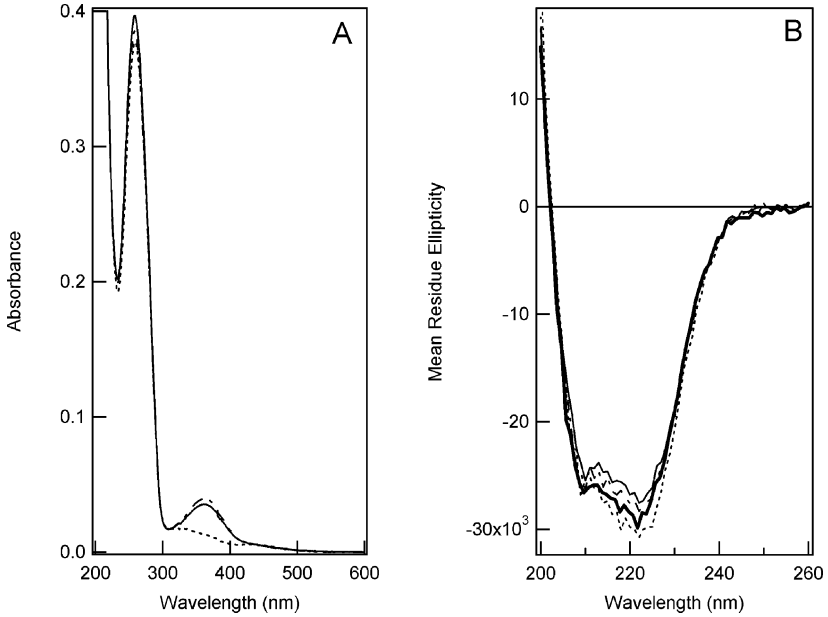

FIGURE 5: Spectroscopic analysis of AZO(*i*, *i* + 7) GCN4-bZIP with AP1 DNA. (A) UV spectra of AZO(*i*, *i* + 7) GCN4-bZIP in the dark-adapted state (solid line) and irradiated state (dotted line) and after recovery (dash−dot line). (B) CD spectra of dark-adapted AZO(*i*, *i* + 7) GCN4-bZIP (solid line), after irradiation (dotted line), and after recovery (dash−dot line). The CD spectrum of wild-type GCN4-bZIP (heavy solid line) is shown for reference. Solution conditions: 10 mM phosphate buffer, pH 7.0, and 50 mM NaCl at 10 ± 1 °C at a protein concentration of 20 μM and AP1 concentration of 20 μM (duplex).

longer than the half-life for thermal reisomerization to the dark-adapted form even at low temperatures. The observed CD change was fully reversible. Incubation of the sample in the dark at 37 °C for 1 h restored the trans spectrum (Figure 3B).

Interaction of Azobenzene Cross-Linked GCN4 with Target DNA. Since DNA binding by GCN4-bZIP is dependent on dimerization (*19*), we then investigated the conformational properties of the modified protein in the presence of target (AP1) DNA. Figure 5A shows UV spectra of dark-adapted (trans) and irradiated (370 nm, ∼1 mW, 5 min) protein solutions in the presence a 2-fold excess of target DNA. The percentage of cis AZO(*i*, *i* + 7) GCN4-bZIP present in the irradiated sample can be calculated to be ∼70% on the basis of a comparison to the spectrum of the pure cis chromophore. As before, the rate of recovery of the trans conformation of AZO(*i*, *i* + 7) GCN4-bZIP in the dark was studied at 25 and 37 °C. These temperatures are below the melting temperature of the AP1 target oligonucleotide (45 °C). Single exponential recovery curves were observed in each case with half-lives similar to those measured in the absence of DNA (Table 1).

CD spectra of irradiated and dark-adapted states of AZO(*i*, *i* + 7) GCN4-bZIP are shown in Figure 5B together with the spectrum for wild-type GCN4-bZIP. The increase in the strength of the signal at 222 nm that is observed with wild-type GCN4-bZIP upon addition of target DNA has been attributed to folding of the basic helices (*17*, *36*). The spectrum of irradiated AZO(*i*, *i* + 7) GCN4-bZIP is closely similar to the wild-type spectrum under these conditions, suggesting that the structure of the DNA-bound cis AZO(*i*, *i* + 7) GCN4-bZIP protein is similar to that of the wild type. The concentrations of protein and DNA employed in the CD experiment (∼20 μM) are orders of magnitude higher than normally employed in DNA-binding assays with GCN4. Interactions would have to have dissociation constants in the millimolar range in order not to be observed under these conditions. The CD spectrum of the dark-adapted (trans) AZO(*i*, *i* + 7) GCN4-bZIP in the presence of target DNA does show increased helicity compared to the DNA-free case (Figure 3B). However, the dark-adapted protein is clearly less helical than the irradiated species, indicating either a reduced affinity for DNA or a distortion of the DNA-bound structure or both.

To measure DNA binding directly, we performed kinetic capillary electrophoresis (CE) measurements (*38*, *39*). This technique is particularly advantageous for assaying light-modulated DNA-binding activity since all manipulations can be performed robotically in the dark under temperature-controlled conditions. Ambient light and temperature changes during sample manipulation are more difficult to control in conventional gel-based electrophoretic mobility shift assays.

We prepared a fluorescein-labeled version of the target AP1 DNA sequence and mixed this with AZO(*i*, *i* + 7) GCN4-bZIP in various ratios. Duplicate samples were either irradiated at 370 nm for 5 min or not and then immediately placed in the sample chamber of the CE instrument at 4 °C in the dark. At this temperature, thermal reversion is sufficiently slow that little cis-to-trans isomerization occurs during the time of the CE measurement. Free and bound DNA are separated and detected by laser-induced fluorescence. Although the (488 nm argon ion) laser may cause some cis-to-trans isomerization, this will not affect the determination of DNA binding since bound and free species have already been separated.

Figure 6 shows typical CE chromatograms. As expected from the CD measurements, the dark-adapted AZO(*i*, *i* + 7) GCN4-bZIP does show some affinity for target DNA; however, irradiation increases this affinity substantially (Figure 6A). Note that the observed change in fraction bound with irradiation is protein concentration dependent. The largest difference is seen at low fractions bound, and the

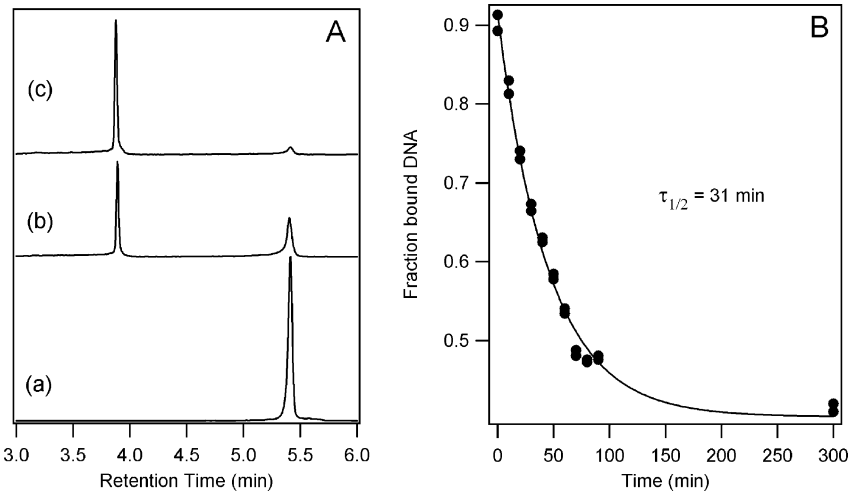

FIGURE 6: Kinetic capillary electrophoresis analysis of AZO(*i*, *i* + 7) GCN4-bZIP with AP1 DNA. (A) CE traces showing (a) AP1 DNA alone (50 nM) in MOPS buffer (pH 7.5), (b) plus 1 μM AZO(*i*, *i* + 7) GCN4-bZIP before irradiation and (c) after irradiation (5 min, 370 nm). Trace b is recovered after thermal relaxation. (B) Time course of thermal relaxation at 25 °C as measured by calculating the fraction of bound DNA vs time after irradiation.

difference disappears with large excesses of protein. Equation 1, which describes all or nothing binding (i.e., an equilibrium between free monomers and bound dimers), has been widely used to describe DNA binding by GCN4-bZIP (*23*, *24*, *40*):

$$f = r\left(\frac{[\text{protein}]^2}{K_d + [\text{protein}]^2}\right) \quad (1)$$

where *f* is the fraction of target DNA bound and *r* represents the maximum fraction bound (>0.95 in all cases) and K_d is the dissociation constant of the dimer−DNA complex. If one assumes that the percentage conversion to the cis isomer after irradiation is similar to that observed during UV and CD measurements (~70% cis), and if one assumes that heterodimeric complexes (i.e., a dimer of one cis and one trans isomer) do not form, then one can use CE data like that shown in Figure 6 to calculate that the dissociation constant (K_d) for the complex decreases approximately 20-fold upon irradiation. Enhanced affinity is observed even in the presence of an ~10000-fold molar excess of nonspecific DNA, although the fold change upon irradiation is diminished. For all cases, incubation of the samples in the dark to allow thermal reversion completely reversed the observed change in DNA-binding affinity. The time course of this relaxation at 25 °C (Figure 6) matches the relaxation observed via UV−vis measurements (Table 1).

DISCUSSION

Vinson and co-workers have shown that, by altering the helical propensity of the coiled-coil domain, DNA binding of bZIP proteins can be altered (*41*, *42*). Increased helical propensity favors dimerization and DNA binding. We installed an intramolecular azobenzene cross-linking unit via coupling to two Cys residues introduced at f positions in the coiled-coil region of the GCN4-bZIP sequence. We expected that the azobenzene cross-linker should directly affect the stability of the AZO(*i*, *i* + 7) GCN4-bZIP coiled coil since it has been observed to have strong effects on the helicity of a variety of peptides (*8*).

As predicted, the dark-adapted AZO(*i*, *i* + 7) GCN4-bZIP showed decreased helicity and decreased DNA-binding affinity in comparison to wild-type GCN4-bZIP. Upon irradiation of AZO(*i*, *i* + 7) GCN4-bZIP, an increase in helical content, as judged by CD analysis, and an increase (~20-fold) in DNA-binding affinity occur (Figures 3, 5, and 6). A larger change in DNA binding for the same relative protein concentration might be achieved by altering the location in the sequence of the Cys residues, their spacing, and/or the number of azobenzene cross-links introduced. In particular, modulation of helix content in the DNA-binding region of helical transcription factors can lead to very substantial changes in binding affinity (*43*, *44*). We note, however, that a comparable change in DNA binding measured in vitro was shown by Vinson et al. to result in measurable changes in the expression of a reporter gene in vivo (*42*).

We note also that the apparent affinity of irradiated AZO(*i*, *i* + 7) GCN4-bZIP is less than wild-type GCN4-bZIP measured under the same conditions by approximately a factor of 10 (data not shown). This is partly due to the incomplete conversion to the cis form upon irradiation but may also be due to partial oxidation of Met residues observed during the production of cross-linked protein. Site-specific mutations designed to avoid oxidation and increase the stability of the cis form of the protein (*35*, *45*) may permit a more "wild-type-like" protein to be produced upon irradiation.

Importantly, the enhanced DNA-binding ability of cis-AZO(*i*, *i* + 7) GCN4-bZIP was fully thermally reversible; the half-life of the cis form in the presence of DNA was actually slightly less than in the absence of DNA (Table 1). This behavior distinguishes a photoswitchable system, comparable to those found in nature, from a phototriggered ("caged") system. The observed reversibility of this system contrasts with the observations of Mascarenas and colleagues, who used an azobenzene cross-linker to link the basic helices of GCN4 directly. In that case, DNA binding prevented the cis-to-trans isomerization (*20*). One source of the difference in the apparent reversibility of the two systems may be the nature of the chromophore used in each case. Although both systems employed azobenzene derivatives, the amide-substituted azobenzene derivatives used here have substan-

tially smaller thermal barriers for isomerization. A second difference is that, in the present case, two chromophores are present per bound complex rather than one; this feature may mean that any tendency of the bound complex to inhibit thermal isomerization is spread over two N═N bonds instead of one.

The loss of reversibility observed by Mascarenas and colleagues parallels observations by Nakayama et al. with an azo-modified *Bam*HI (*46*) enzyme as well as earlier work by Shinkai and colleagues (*47*, *48*), who studied the behavior of azobenzene derivatives functionalized with crown ethers and other metal ion-binding groups. The cis forms of these compounds bind their targets (metal ions) via electrostatic interactions and bind with higher affinity than the trans forms. In most cases, however, strong target binding also inhibits the thermal and photochemical cis → trans isomerization process (i.e., the reversibility of the system) just as is observed with the Mascarenas system. In the colloid and polymer literature, inhibition of thermal cis-to-trans isomerization of azobenzene has also been reported (e.g., ref *49*) and attributed to dense packing around azobenzene units and a decrease in the "free volume" around the chromophore.

In molecular terms, the key criterion for reversibility would appear to be the accessibility of the transition state for isomerization when the chromophore is attached to the target (protein, polymer, or other). Since the three-dimensional structure of the GCN4-bZIP/DNA complex is known at atomic resolution, one can attempt to estimate the accessibility of the relevant transition state. Any such attempt is complicated by the fact that there does not appear to be general agreement on the precise mechanism for azobenzene isomerization (i.e., rotation vs inversion). Figure 7 shows models of transition states for both processes. If one fixes the geometry of the azo unit at one or other of the possible transition state structures, systematic rotation of all of the single bonds in the compounds gives the range of sulfur-to-sulfur distances (the attachment point to the protein) that are compatible with transition state formation for each case (Figure 7).

If one measures the distance between γ atoms of the side chains of residues 262 and 269 in the GCN4-bZIP/DNA X-ray crystal structure, one obtains values of 11.4 and 10.2 Å for the two protein chains. Jelezarov and colleagues have carried out all-atom molecular dynamics simulation of the coiled-coil domain of GCN4 with explicit solvent (*30*). Analysis of these molecular dynamics trajectories as described in the Materials and Methods section shows that the distance between γ atoms of the side chains of residues 262 and 269 varies between about 9.5 and 13.5 Å with a most probable value of 11.2 Å. This range is similar to what one obtains by simply rotating the $\chi 1$ side-chain torsion angle of residues 262 and 269. This distance range partially overlaps the distance range compatible with an inversional transition state of the cross-linker (13−18.5 Å) (Figure 7) and overlaps substantially with the distance range compatible with a rotational transition state of the cross-linker (11−17.5 Å) (Figure 7). Interestingly, recent computational evidence has suggested the rotational mechanism is preferred for azobenzene isomerization (*50*). In either case, the structure of the GCN4-bZIP DNA complex does not prevent access to transition states required for isomerization, a key requirement for full reversibility.

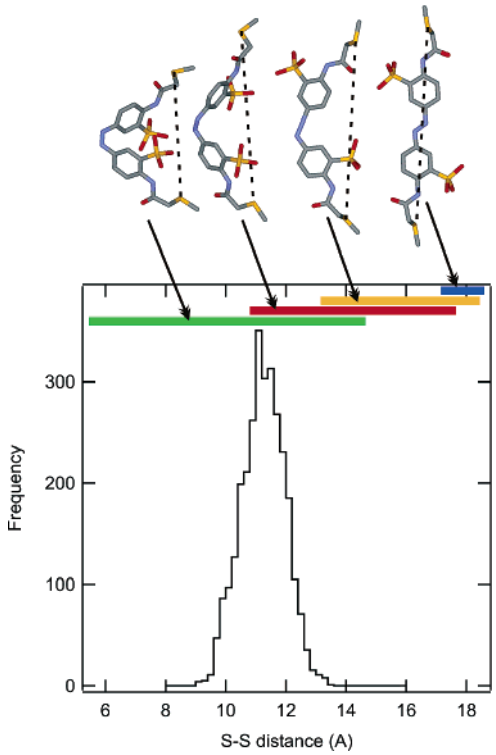

FIGURE 7: Compatibility of Cys S−S distances in the GCN4 leucine zipper region with S−S distances in the cross-linker. A histogram of distances between side-chain γ atoms of residues 262 and 269 in the leucine zipper domain of wild-type GCN4-p1 during ~1 ns of molecular dynamics at 298 K. (Above) Sample structures of the azobenzene cross-linker in cis, rotational transition state, inversional transition state, and trans conformations (from left to right). The distance ranges (between S atoms indicated by dotted lines) accessible via single bond rotations in each of these structures are indicated (cis state, green; rotational transition state, red; inversional transition state, orange; trans state, blue).

It is difficult to perform the same sort of structural analysis of the DNA−protein complex studied by Mascarenas and colleagues since one cannot safely assume that the much more substantial modifications made to the GCN4-bZIP sequence caused no major change in the three-dimensional structure. In the Mascarenas case, the bZIP sequences are truncated at residue 248 and then linked together via a Gly-Gly-Cys-AZO-Cys-Gly-Gly unit (*20*). It is surprising that what appears to be a fairly flexible linking unit does not appear to provide sufficient flexibility for the transition state to be easily accessed in this system. However, these authors report that the corresponding peptide without the pairs of Gly residues was unable to bind to DNA at all in either the cis or trans form (*20*), suggesting that conformational demands placed on the linker in their system were, in fact, quite severe. It would be interesting, therefore, to test whether adding more flexibility to the linker in the Mascarenas design would allow reversibility. Of course, too much flexibility would be expected to abrogate any difference between cis and trans isomers.

The relative simplicity of this system compared to naturally occurring photosensitive proteins such as rhodopsins and phytochromes may permit detailed study of how a localized conformational event (isomerization of one bond) can be transmitted effectively throughout a functional protein. Indeed, Sporlein et al. have shown that the conformational dynamics of such systems after a light-triggered isomeriza-

tion event are amenable to study by all-atom molecular dynamics simulations (*51*). Such data may be combined with extensive theoretical and experimental data on the folding of helical coiled coils (e.g., ref *52*) to generate a relatively complete picture of protein photocontrol.

In addition to providing a tractable model for probing the molecular mechanism of reversible photoregulation in proteins, these photoregulated DNA-binding protein systems may lead to practical tools for the study of cellular chemistry. Several groups have reported that basic zipper domains and/or cross-linked peptide species similar to the construct described here can be taken up spontaneously by eukaryotic cells (*53*, *54*) or, alternatively, such constructs could be modified to include cell-penetrating sequences to permit cellular uptake (*55*). Minimal DNA-binding proteins such as the GCN4 construct described here may be used to bind to AP-1 target sequences and inhibit function of endogenous AP-1 binding proteins. Photocontrolled GCN4 analogues may therefore permit external control of transcriptional processes. Engineered photocontrol of transcription offers numerous advantages over conventional inducible gene expression systems (*56*−*58*).

ACKNOWLEDGMENT

We are grateful to Prof. Martha Oakley for the donation of GCN4-bZIP wild-type plasmid and to Dr. Ilian Jelezarov for sharing his GCN4 p1 MD trajectories.

REFERENCES

1. Adams, S. R., and Tsien, R. Y. (1993) Controlling cell chemistry with caged compounds, *Annu. Rev. Physiol. 55*, 755−784.
2. Curley, K., and Lawrence, D. S. (1999) Light-activated proteins, *Curr. Opin. Chem. Biol. 3*, 84−88.
3. Thompson, S. M., Kao, J. P., Kramer, R. H., Poskanzer, K. E., Silver, R. A., Digregorio, D., and Wang, S. S. (2005) Flashy science: controlling neural function with light, *J. Neurosci. 25*, 10358−10365.
4. Shigeri, Y., Tatsu, Y., and Yumoto, N. (2001) Synthesis and application of caged peptides and proteins, *Pharmacol. Ther. 91*, 85−92.
5. Schafer, E., and Bowle, C. (2002) Phytochrome-mediated photoperception and signal transduction in higher plants, *EMBO Rep. 3*, 1042−1048.
6. Genick, U. K., Soltis, S. M., Kuhn, P., Canestrelli, I. L., and Getzoff, E. D. (1998) Structure at 0.85 Å resolution of an early protein photocycle intermediate, *Nature 392*, 206−209.
7. DeGrado, W. F., Wasserman, Z. R., and Lear, J. D. (1989) Protein design, a minimalist approach, *Science 243*, 622−628.
8. Woolley, G. A. (2005) Photocontrolling peptide alpha helices, *Acc. Chem. Res. 38*, 486−493.
9. Kumita, J. R., Smart, O. S., and Woolley, G. A. (2000) Photocontrol of helix content in a short peptide, *Proc. Natl. Acad. Sci. U.S.A. 97*, 3803−3808.
10. Flint, D. G., Kumita, J. R., Smart, O. S., and Woolley, G. A. (2002) Using an azobenzene cross-linker to either increase or decrease peptide helix content upon trans-to-cis photoisomerization, *Chem. Biol. 9*, 391−397.
11. Borisenko, V., and Woolley, G. A. (2005) Reversibility of conformational switching in light-sensitive peptides, *J. Photochem. Photobiol., A. 173*, 21−28.
12. O'Shea, E. K., Rutkowski, R., and Kim, P. S. (1989) Evidence that the leucine zipper is a coiled coil, *Science 243*, 538−542.
13. Hill, D. E., Hope, I. A., Macke, J. P., and Struhl, K. (1986) Saturation mutagenesis of the yeast his3 regulatory site: requirements for transcriptional induction and for binding by GCN4 activator protein, *Science 234*, 451−457.
14. Arndt, K., and Fink, G. R. (1986) GCN4 protein, a positive transcription factor in yeast, binds general control promoters at all 5′ TGACTC 3′ sequences, *Proc. Natl. Acad. Sci. U.S.A. 83*, 8516−8520.
15. O'Shea, E. K., Klemm, J. D., Kim, P. S., and Alber, T. (1991) X-ray structure of the GCN4 leucine zipper, a two-stranded, parallel coiled coil, *Science 254*, 539−544.
16. Landschulz, W. H., Johnson, P. F., and McKnight, S. L. (1988) The leucine zipper: A hypothetical structure common to a new class of DNA binding proteins, *Science 240*.
17. Weiss, M. A., Ellenberger, T., Wobbe, C. R., Lee, J. P., Harrison, S. C., and Struhl, K. (1990) Folding transition in the DNA-binding domain of GCN4 on specific binding to DNA, *Nature 347*, 575−578.
18. Bracken, C., Carr, P. A., Cavanagh, J., and Palmer, A. G., III (1999) Temperature dependence of intramolecular dynamics of the basic leucine zipper of GCN4: implications for the entropy of association with DNA, *J. Mol. Biol. 285*, 2133−2146.
19. Ellenberger, T. E., Brandl, C. J., Struhl, K., and Harrison, S. C. (1992) The GCN4 basic region leucine zipper binds DNA as a dimer of uninterrupted alpha helices: crystal structure of the protein−DNA complex, *Cell 71*, 1223−1237.
20. Caamano, A. M., Vazquez, M. E., Martinez-Costas, J., Castedo, L., and Mascarenas, J. L. (2000) A light-modulated sequence-specific DNA-binding peptide, *Angew. Chem., Int. Ed. Engl. 39*, 3104−3107.
21. Cuenoud, B., and Schepartz, A. (1993) Design of a metallo-bZIP protein that discriminates between CRE and AP1 target sites: selection against AP1, *Proc. Natl. Acad. Sci. U.S.A 90*, 1154−1159.
22. Aizawa, Y., Sugiura, Y., Ueno, M., Mori, Y., Imoto, K., Makino, K., and Morii, T. (1999) Stability of the dimerization domain effects the cooperative DNA binding of short peptides, *Biochemistry 38*, 4008−4017.
23. Hollenbeck, J. J., and Oakley, M. G. (2000) GCN4 binds with high affinity to DNA sequences containing a single consensus half-site, *Biochemistry 39*, 6380−6389.
24. Bird, G. H., Lajmi, A. R., and Shin, J. A. (2002) Sequence-specific recognition of DNA by hydrophobic, alanine-rich mutants of the basic region/leucine zipper motif investigated by fluorescence anisotropy, *Biopolymers 65*, 10−20.
25. Kumita, J. R., Flint, D. G., Smart, O. S., and Woolley, G. A. (2002) Photo-control of peptide helix content by an azobenzene cross-linker: steric interactions with underlying residues are not critical, *Protein Eng. 15*, 561−569.
26. Brown, C. J. (1966) A refinement of the crystal structure of azobenzene, *Acta Crystallogr. 21*, 146−152.
27. Robertson, J. M. (1939) Crystal structure and configuration of the isomeric azobenzenes, *J. Chem. Soc.*, 232−236.
28. Fliegl, H., Kohn, A., Hattig, C., and Ahlrichs, R. (2003) Ab initio calculation of the vibrational and electronic spectra of trans- and cis-azobenzene, *J. Am. Chem. Soc. 125*, 9821−9827.
29. Ikegami, T., Kurita, N., Sekino, H., and Ishikawa, Y. (2003) Mechanism of cis-to-trans isomerization of azobenzene: A direct MD study, *J. Phys. Chem. A 107*, 4555−4562.
30. Gorfe, A. A., Ferrara, P., Caflisch, A., Marti, D. N., Bosshard, H. R., and Jelesarov, I. (2002) Calculation of protein ionization equilibria with conformational sampling: p*K*(a) of a model leucine zipper, GCN4 and barnase, *Proteins 46*, 41−60.
31. Bairoch, A., and Apweiler, R. (2000) The SWISS-PROT protein sequence database and its supplement TrEMBL in 2000, *Nucleic Acids Res. 28*, 45−48.
32. Kumita, J. R., Flint, D. G., Woolley, G. A., and Smart, O. S. (2003) Achieving photo-control of protein conformation and activity: producing a photo-controlled leucine zipper, *Faraday Discuss. 122*, 89−103 (discussion 171−190).
33. Weiner, S. J., Kollman, P. A., Case, D. A., Singh, U. C., Ghio, C., Alagona, G., Profeta, S., Jr., and Weiner, P. (1984) A new force field for molecular mechanical simulation of nucleic acids and proteins, *J. Am. Chem. Soc. 106*, 765−784.
34. Zhang, Z., Burns, D. C., Kumita, J. R., Smart, O. S., and Woolley, G. A. (2003) A water-soluble azobenzene cross-linker for photocontrol of peptide conformation, *Bioconjugate Chem. 14*, 824−829.
35. Ibarra-Molero, B., Zitzewitz, J. A., and Matthews, C. R. (2004) Salt-bridges can stabilize but do not accelerate the folding of the homodimeric coiled-coil peptide GCN4-p1, *J. Mol. Biol. 336*, 989−996.
36. Weiss, M. A. (1990) Thermal unfolding studies of a leucine zipper domain and its specific DNA complex: implications for scissor's grip recognition, *Biochemistry 29*, 8020−8024.

37. Meng, F. G., Zeng, X., Hong, Y. K., and Zhou, H. M. (2001) Dissociation and unfolding of GCN4 leucine zipper in the presence of sodium dodecyl sulfate, *Biochimie 83*, 953−956.
38. Petrov, A., Okhonin, V., Berezovski, M., and Krylov, S. N. (2005) Kinetic capillary electrophoresis (KCE): a conceptual platform for kinetic homogeneous affinity methods, *J. Am. Chem. Soc. 127*, 17104−17110.
39. Berezovski, M., and Krylov, S. N. (2005) Thermochemistry of protein-DNA interaction studied with temperature-controlled non-equilibrium capillary electrophoresis of equilibrium mixtures, *Anal. Chem. 77*, 1526−1529.
40. Berger, C., Piubelli, L., Haditsch, U., and Bosshard, H. R. (1998) Diffusion-controlled DNA recognition by an unfolded, monomeric bZIP transcription factor, *FEBS Lett. 425*, 14−18.
41. Szilak, L., Moitra, J., Krylov, D., and Vinson, C. (1997) Phosphorylation destabilizes alpha-helices, *Nat. Struct. Biol. 4*, 112−114.
42. Szilák, L., Moitra, J., and Vinson, C. (1997) Design of a leucine zipper coiled coil stabilized 1.4 kcal mol^{-1} by phosphorylation of a serine in the e position, *Protein Sci. 6*, 1273−1283.
43. Guerrero, L., Smart, O. S., Woolley, G. A., and Allemann, R. K. (2005) Photocontrol of DNA binding specificity of a miniature engrailed homeodomain, *J. Am. Chem. Soc. 127*, 15624−15629.
44. Guerrero, L., Smart, O. S., Weston, C. J., Burns, D. C., Woolley, G. A., and Allemann, R. K. (2005) Photochemical regulation of DNA-binding specificity of MyoD, *Angew. Chem., Int. Ed. Engl. 44*, 7778−7782.
45. O'Neil, K. T., and DeGrado, W. F. (1990) A thermodynamic scale for the helix-forming tendencies of the commonly occurring amino acids, *Science 250*, 646−651 [erratum: (1991) *Science 253*, 952].
46. Nakayama, K., Endo, M., and Majima, T. (2004) Photochemical regulation of the activity of an endonuclease BamHI using an azobenzene moiety incorporated site-selectively into the dimer interface, *Chem. Commun.*, 2386−2387.
47. Shinkai, S. (1990) Functionalization of crown ethers and calixarenes: New applications as ligands, carriers, and host molecules, in *Bioorganic Chemistry Frontiers* (Dugas, H., Ed.) pp 161−195, Springer-Verlag, Berlin.
48. Shinkai, S., Nakamura, S., Nakashima, M., Manabe, O., and Iwamoto, M. (1985) Photoresponsive crown ethers. 16. Photoregulated ion-binding to azobenzene-linked ethylenediamines and iminodiacetic acids, *Bull. Chem. Soc. Jpn. 58*, 2340−2347.
49. Takahashi, M., Okuhara, T., Yokohari, T., and Kobayashi, K. (2005) Effect of packing on orientation and cis−trans isomerization of azobenzene chromophore in Langmuir−Blodgett film, *J. Colloid Interface Sci*. (in press).
50. Tiago, M. L., Ismail-Beigi, S., and Louie, S. G. (2005) Photoisomerization of azobenzene from first-principles constrained density-functional calculations, *J. Chem. Phys. 122*, 094311.
51. Sporlein, S., Carstens, H., Satzger, H., Renner, C., Behrendt, R., Moroder, L., Tavan, P., Zinth, W., and Wachtveitl, J. (2002) Ultrafast spectroscopy reveals subnanosecond peptide conformational dynamics and validates molecular dynamics simulation, *Proc. Natl. Acad. Sci. U.S.A. 99*, 7998−8002.
52. Wang, T., Lau, W. L., DeGrado, W. F., and Gai, F. (2005) T-jump infrared study of the folding mechanism of coiled-coil GCN4-p1, *Biophys. J. 89*, 4180−4187.
53. Walensky, L. D., Kung, A. L., Escher, I., Malia, T. J., Barbuto, S., Wright, R. D., Wagner, G., Verdine, G. L., and Korsmeyer, S. J. (2004) Activation of apoptosis in vivo by a hydrocarbon-stapled BH3 helix, *Science 305*, 1466−1470.
54. Futaki, S. (2005) Membrane-permeable arginine-rich peptides and the translocation mechanisms, *Adv. Drug Deliv. Rev. 57*, 547−558.
55. Kawamura, K. S., Sung, M., Bolewska-Pedyczak, E., and Gariepy, J. (2006) Probing the impact of valency on the routing of arginine-rich peptides into eukaryotic cells, *Biochemistry 45*, 1116−1127.
56. Shimizu-Sato, S., Huq, E., Tepperman, J. M., and Quail, P. H. (2002) A light-switchable gene promoter system, *Nat. Biotechnol. 20*, 1041−1044.
57. Mendelsohn, A. R. (2002) An enlightened genetic switch, *Nat. Biotechnol. 20*, 985−987.
58. Asanuma, H., Tamaru, D., Yamazawa, A., Liu, M., and Komiyama, M. (2002) Photoregulation of the transcription reaction of T7 RNA polymerase by tethering an azobenzene to the promoter, *ChemBioChem 3*, 786−789.

BI060142R